Opinion Article

Application of SEM and XRD in the microstructure analysis of fiber-reinforced concrete corroded by salt solution

Abstract: In order to study the damage law of salt solution erosion on the microstructure of concrete, the dry wet alternation method was used to conduct salt solution corrosion tests on the samples. The corrosion characteristics and mechanisms were analyzed from macroscopic experiments such as corrosion results, relative dynamic elastic modulus, and mass loss rate; Then, SEM and XRD were used to further demonstrate and explain the corrosion mechanism from a microscopic perspective. The conclusion drawn from the analysis: The observation and analysis of the erosion products and SEM and XRD microscopic characteristics of fiber-reinforced concrete indicate that in the initial state without erosion, the sample contains original cracks and pores, and the fibers are tightly bound to the cement slurry. Under the acceleration of dry wet cycles, sulfate erosion is mainly gypsum type erosion and ettringite type erosion, and the erosion products are columnar and needle shaped distribution of ettringite and gypsum crystals; In the later stage of erosion, the surface concrete deteriorates severely, the cement slurry gradually falls off, the internal pores increase, and cracks increase, resulting in partial separation of fibers from the cement slurry. At this time, the fibers rely on their own tensile strength to play a role in toughening and crack resistance.

Keywords: salt solution, concrete erosion, Fibers, Corrosion, SEM and XRD Methods

1. INTRODUCTION

Concrete is widely used in engineering fields such as national defense, transportation, civil construction, and water conservancy due to its excellent durability, high compressive strength, good workability, and ease of structural deformation control. The durability of concrete has always been a concern in the engineering and academic fields. The durability of concrete is affected by many environmental factors, such as freeze-thaw failure, carbonization, sulfate corrosion, alkali aggregate reaction, etc[1]. The distribution area of sulfate corrosion environment in China is relatively wide, which is a common form of deterioration of concrete structures. Concrete structures located in the water level fluctuation zone are also affected by the wet dry cycle. Under the synergistic effect of sulfate and wet dry cycle, the corrosion deterioration rate and process of concrete structures will be accelerated, and the durability loss of concrete will be more significant[2].

Ordinary plain concrete has high brittleness and poor durability, and the existence of internal interface transition zones in the concrete matrix greatly affects the

mechanical properties and durability of concrete. The mechanical properties of concrete mixed with fibers have been greatly improved. Fibers can form a stable spatial network structure inside the concrete, improve the stress redistribution inside the concrete, and change its failure mode. Basalt fibers passing through the weak interface zone can enhance the mechanical stability of the interface transition zone, improve the microstructure of the concrete, and improve the mechanical properties of the concrete. Previous studies have achieved significant results in analyzing the erosion effect of salt solutions on the internal structure of concrete[3,4,5,6]. The methods commonly used include mercury intrusion experiments, scanning electron microscopy experiments, X-ray diffraction experiments, and CT scanning experiments. This article mainly discusses the application of scanning electron microscopy and X-ray diffraction experiments in the erosion of concrete microstructures by salt solutions.

2. Methodology:

2.1 Method

After the concrete specimens are cured, the sulfate corrosion test is conducted using the wet dry alternation method, which simulates the corrosion damage phenomenon of the internal structure of concrete by repeatedly cycling wet dry cycles in a solution. The specific method is to immerse the concrete specimen in a composite salt solution for 10 hours, and the concentrations of Na_2SO_4 and NaCl in the salt solution depend on the concentration of Cl^- and SO_4^{2-} ions in the local water. Remove the test piece from the solution, wipe it clean, and air dry for 1 hour. Then place the test piece in a constant temperature drying oven at 60 ℃ for 12 hours. After that, remove the test piece and cool it at room temperature for 1 hour as one cycle, ensuring that each cycle is 24 hours[7]. Each experiment is conducted for 30 cycles, during which macroscopic experiments such as dynamic elastic modulus and mass determination can be carried out. At the end of the 30th cycle, samples of corrosion products from specimens with typical salt corrosion diseases are taken, and microstructure analysis experiments such as SEM scanning electron microscopy and XRD diffraction analysis are carried out[8].

2.2 SEM Principle

Scanning electron microscope (SEM) is an observation technique that falls between transmission electron microscope and optical microscope. It uses a focused narrow high-energy electron beam to scan the sample, and through the interaction between the beam and the material, it excites various physical information. The collection, amplification, and re imaging of this information are used to achieve the purpose of characterizing the microscopic morphology of the material. The resolution of the new scanning electron microscope can reach 1nm; The magnification can be continuously adjustable up to 300000 times or more; And the scenery is deep, the field of view is large, and the imaging stereo effect is good [9]. In addition, by combining scanning electron microscopy with other analytical instruments, it is possible to observe the microstructure while conducting material micro area composition analysis. For example, combining scanning electron microscopy and X-ray diffraction analysis can further infer the specific phase of the imaging [10].

2.3 SEM Analysis

After the strength test, the specimen is crushed, and a thin slice of concrete near the surface of the specimen is selected to terminate hydration by placing it in anhydrous ethanol to prepare the test sample. The microstructure changes of the specimen after corrosion are observed using a Hitachi S4800 cold field emission scanning electron microscope (FESEM-EDS) from Japan.

2.4 XRD Principle

The basic principle of X-ray diffraction is that when a monochromatic X-ray beam is incident on a crystal, the crystal is composed of a regular arrangement of atoms arranged in a unit cell. The distance between these regularly arranged atoms is of the same order of magnitude as the wavelength of the incident X-ray in X-ray diffraction analysis. Therefore, X-rays scattered by different atoms interfere with each other, producing strong X-ray diffraction in certain special directions. The orientation and intensity of the diffraction lines in spatial distribution are closely related to the crystal structure, and the diffraction patterns produced by each crystal reflect the atomic distribution law inside the crystal. The fundamental basis for X-ray diffraction analysis is the Bragg equation [11]:

$$2d_{hkl}\sin\theta_{hkl} = n\lambda$$

In the formula: d is the interplanar spacing; N is the diffraction order; hkl is the diffraction index.

The most basic data obtained from X-ray diffraction are diffraction angle values and intensity values. Different structural elements of a substance can be obtained and calculated from the three elements of diffraction peaks. 1. Peak position - qualitative phase analysis, determination of crystal system, indexing, calculation of cell parameters, etc. 2. Peak intensity - calculate the phase content and crystallinity. 3. Peak shape - estimate the degree of crystallinity and calculate the grain size. The principle of qualitative phase analysis is to determine the corresponding unknown phase by comparing a set of experimental data with known standard cards. The specific steps are: data import, background detection and processing, peak searching, automatic database retrieval, listing of candidate phases, manual screening and confirmation.

2.4 XRD Analysis

After the corresponding erosion cycle is completed, the test piece is dried for 48 hours. Then, a concrete single-sided grinder is used to collect powder in layers, with a layer of every 2mm within 20mm from the surface of the concrete. The powder is sieved using a square hole sieve with a nominal diameter of 0.16mm. The sieved powder is placed in an oven at a temperature of 105 ± 5 for 2 hours, taken out, and cooled to room temperature in a dryer for later use [12]. The XRD pattern of the corrosion specimen product was determined using a Japanese Rigaku D/MAX2400 X-ray diffractometer, and its phase composition was analyzed using Jade6.5 phase analysis software with a scanning range of 5-45.

3. RESULTS AND DISCUSSION

3.1 Macroscopic Phenomena

In the case of salt solution corrosion, there was a significant increase in voids and exposure of coarse aggregates at the edges and corners of the specimen surface. It is speculated that the main reason for these corrosion damages is the chemical reaction between the cement hydration product calcium hydroxide on the surface of the specimen and the continuously infiltrating corrosive ions, producing unknown corrosion products. These corrosion products accumulate in the pores and cracks on the surface of the specimen, causing the mortar layer on the surface of the specimen to gradually corrode [13]. With the increase of the number of salt corrosion dry wet cycles, the corrosion products in the surface cracks and pores continue to increase, and the expansion stress continues to increase, causing crack propagation and allowing more corrosion solution to enter the interior of the specimen, resulting in corrosion and accelerating the degradation process. However, the concrete mixed with fibers only showed a small amount of mortar layer detachment at the corners and surface, and some specimens showed "salt frost" crystals on the surface, but with few pores and no obvious cracks. The overall appearance was relatively complete, and the ability to resist salt solution erosion and damage was enhanced. Therefore, it can be concluded that the "bridging" effect of fibers between cracks inside the concrete reduces stress concentration at the crack, increases crack propagation resistance, suppresses crack development, and improves the specimen's ability to resist composite salt erosion [14].

In the dynamic modulus of elasticity experiment and mass loss rate test, it was found that under the same erosion conditions, the specimen with added fibers had the greatest relative increase in dynamic modulus of elasticity and could significantly reduce the mass loss rate of the specimen. This also proves that adding fibers to concrete can effectively improve its salt corrosion resistance [15].

3.2 Microstructure Analysis

3.2.1SEM Result Analysis

Under the condition of salt solution erosion, the scanning electron microscopy images of concrete are shown in Figure 1 and Figure 2:

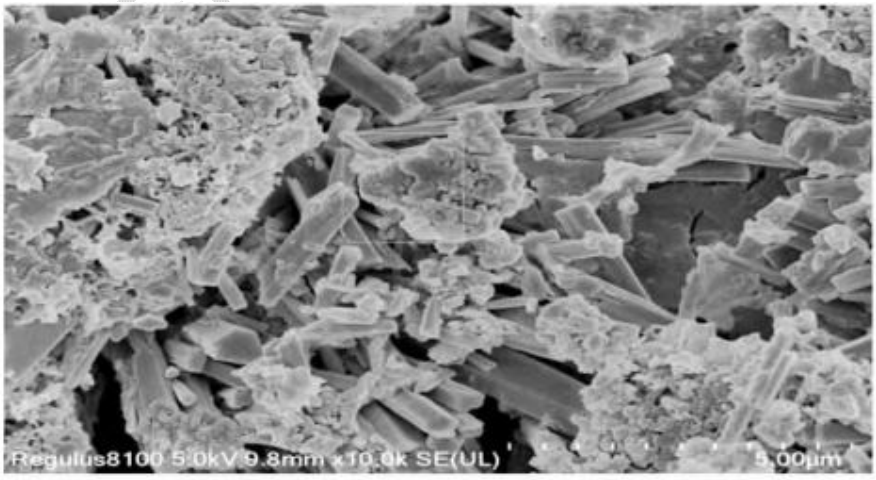

Figure 1 Microstructure characteristics of concrete specimens

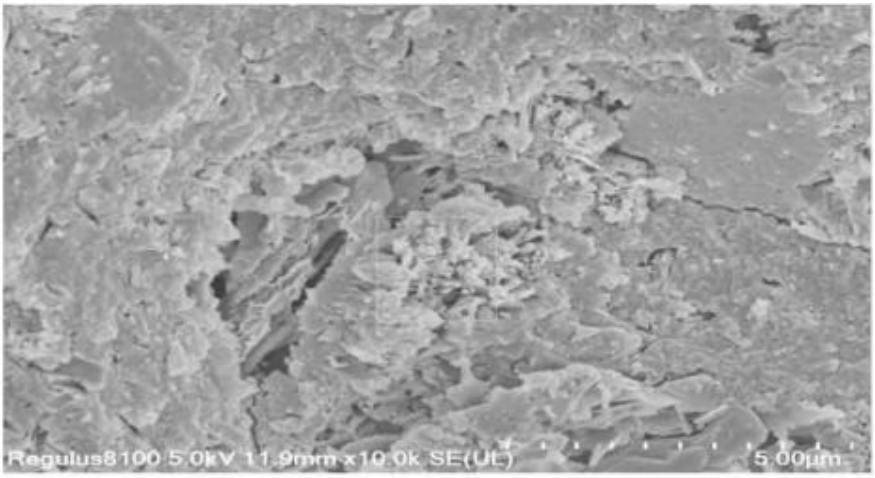

Figure 2 Microstructure characteristics of fiber-reinforced concrete specimens

From Figures 1 and 2, it can be seen that the interior of concrete without fibers is mainly composed of short columnar and needle shaped corrosion products, while the corrosion products between microcracks inside the concrete with fibers are significantly reduced, and most of the areas around the cracks remain dense. This indicates that although the number of wet dry cycles increases, the generation rate of corrosion products is significantly slowed down. This is mainly because the tensile effect of fibers inside the concrete restricts the expansion of cracks to a certain extent, reducing the degree of damage to the concrete when subjected to composite salt erosion [16].

3.2.2 XRD Result Analysis

The XRD diffraction analysis of concrete under salt solution erosion is shown in Figure 3:

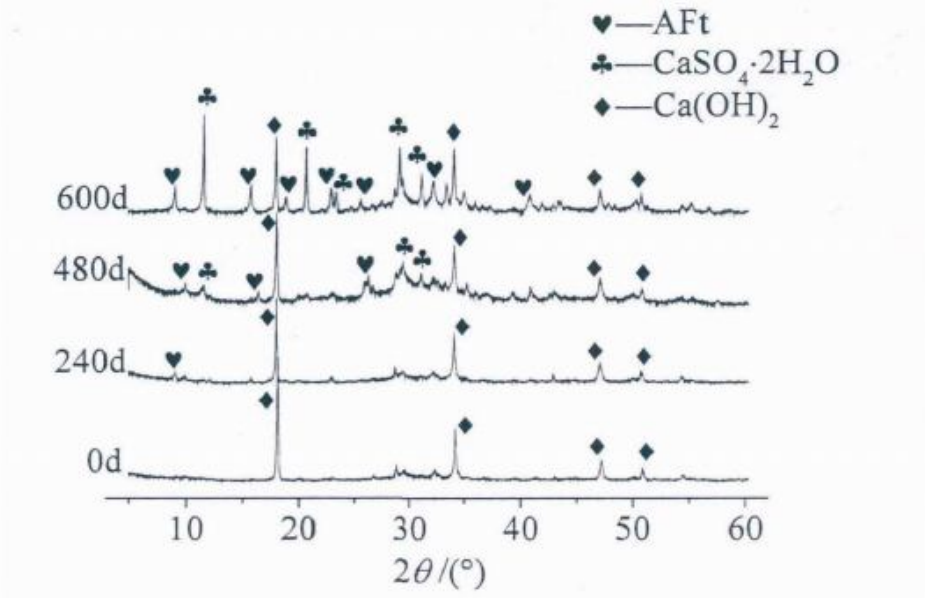

Figure 3 XRD corrosion product diagram of concrete specimens

From Figure 3, it can be seen that before corrosion, the main diffraction peak is calcium hydroxide. After 240 days of corrosion in sodium sulfate solution, the diffraction peak of ettringite appears. After 480 days of corrosion, it can be seen that ettringite and gypsum coexist. After 600 days of corrosion, the diffraction peaks of ettringite near 9, 16, 23, 26, and 32 are observed, and the diffraction peaks of gypsum with higher diffraction intensity near 12, 21, 29, and 31 are observed,Corrosion product ettringite appeared at 240d, new corrosion product gypsum appeared at 480d, and ettringite and gypsum were generated in multiple locations at 600d. It can be seen that the corrosion reaction of ettringite and gypsum occurred simultaneously in the salt solution sample, and with the increase of time, the corrosion reaction continued to intensify, and the quantities of ettringite and gypsum significantly increased [17].

Based on the scanning electron microscopy images and XRD patterns, the final conclusion was drawn that the short columnar and needle shaped corrosion products observed in the scanning electron microscopy images were ettringite and gypsum. When the specimen is in a corrosive environment of salt solution, the change in its performance is divided into two stages with the invasion of sodium sulfate solution: the first stage is the filling and compacting stage, which is due to the reaction between sulfate ions and hydration products to produce corrosion products such as ettringite. These corrosion products fill the original pores inside the specimen, making it denser and increasing its strength; The second stage is the expansion and failure stage, during which a large amount of corrosion products accumulate, and the original pores no longer provide sufficient space. Calcium aluminate contains a large amount of crystal water, which is 1.5 times larger in volume than the original hydrated calcium aluminate. The expansion effect is obvious, and it grows radially in a needle shape, which easily generates large internal stresses, causing the generation of new cracks inside the specimen and the expansion of original cracks. Therefore, the performance of the specimen deteriorates and the strength decreases during this stage. As the corrosion intensifies and the internal cracks are interconnected, the strength continues to decrease [18].

4. Conclusion

This article combines indoor macroscopic testing and microscopic analysis to study the macroscopic morphology, microscopic structure, and erosion products of fiber-reinforced concrete under salt solution erosion, and explores the mechanism of fiber-reinforced concrete's resistance to salt solution erosion. The main conclusions are as follows:

At the initial stage of erosion, the surface and edges of the fiber-reinforced concrete specimens are relatively intact, with only sandification appearing on the surface. As the number of dry wet cycles increases, the deterioration of the concrete specimens becomes apparent, with edges beginning to break, surrounding aggregates partially falling off, surface cracks increasing, and even penetrating cracks appearing. Basalt fiber can not only reduce the internal erosion products of the specimen and weaken the sulfate erosion effect, but also play a bridging and force transmission role inside the specimen, which can to some extent constrain the development and propagation of cracks and alleviate the peeling of the cement slurry on the surface of the

specimen.

Observation and analysis of erosion products and SEM and XRD microscopic characteristics of fiber-reinforced concrete indicate that in the initial state without erosion, basalt fiber-reinforced concrete contains original cracks and pores inside the sample. The fibers are tightly bonded to the cement slurry, and the compactness of the cement slurry around the fibers is improved, filling some of the original defects; Under the accelerated action of dry wet cycles, sulfate erosion mainly includes gypsum type erosion and ettringite type erosion, and the erosion products are columnar and needle shaped distribution of ettringite and gypsum crystals; In the later stage of erosion, the surface concrete deteriorates severely, the cement slurry gradually falls off, the internal pores increase, and cracks increase, resulting in partial separation of fibers from the cement slurry. At this time, the fibers rely on their own tensile strength to play a role in toughening and crack resistance.

Fiber is added to concrete, which improves the performance indicators such as matrix strength and relative dynamic modulus by relying on its high mechanical properties such as tensile strength, stress-strain ratio, and ultimate elongation, thereby enhancing the long-term service performance of concrete. The degradation law of basalt fiber reinforced concrete under the action of sulfate and dry wet cycles is influenced by multiple factors, including the concentration of sulfate solution, the number of dry wet cycles, and the content of basalt fiber. Fibers play a role in strengthening, cracking resistance, and toughening in concrete, and fiber-reinforced concrete has better resistance to sulfate corrosion than plain concrete.

Disclaimer (Artificial intelligence)

Author(s) hereby declare that NO generative AI technologies such as Large Language Models (ChatGPT, COPILOT, etc.) and text-to-image generators have been used during the writing or editing of this manuscript.

References

[1] Nili M,Azarioon.Novel internal-deterioration model of concrete exposed to freeze-thaw cycles[J].Journal of Materials in Civil Engineering,2017,29(9):04017132

[2] Gao J M,Yu Z X,Song L G,et al.Durability of concrete exposed to sulfate attack under flexural loading and drying-wetting cycles[J].Construction and Building Materials,2013,39:33-38

[3] Lin J F.Research on the Mechanical Properties and Microstructure of Basalt Fiber Reinforced Concrete Based on SEM [J] Construction Technology, 2018 (18)

[4] Gao Zhen; Cao Peng; Sun Xinjian; Zhao Yawei .Analysis and Microscopic Characterization of Compressive Strength of Basalt Fiber Reinforced Concrete [J] Journal of Hydroelectric Power Generation, 2018 (08)

[5] Zhang Yongsheng; Li Qingning; Fang Chenze.Research on the Mechanical Properties and Durability of Fiber Reinforced Concrete Based on Microscopic Analysis [J] Concrete, 2016 (08)

[6] Xia Jinxi, Nie Junkun.Study on the microstructure of fiber-reinforced concrete under salt freezing erosion [J] Concrete, 2024 (08)

[7] Experimental study on the resistance of basalt polypropylene fiber reinforced concrete to sulfate dry wet cycles Xin Ming; Wang Xuezhi; Kong Xiangqing; Liu Huaxin; Tong Huan Concrete, 2021

[8] Deterioration mechanism of plain and blended cement mortars partially exposed to sulfate attack. Fei Chen;Jianming Gao;Bing Qi;Daman Shen.Construction and Building Materials,2017

[9] Study on the mechanical properties of basalt fiber reinforced concrete under salt freezing action Xu Cundong; Li Hongfei; Huang Song; Li Zhen; Lian Haidong; Li Zhirui. Hydroelectric Energy Science, 2021

[10] Damage mechanisms of two-stage concrete exposed to chemical and physical sulfate attack. M.F. Najjar;M.L. Nehdi;A.M. Soliman;T.M. Azabi.Construction and Building Materials,2017

[11] The degradation law of basalt fiber reinforced concrete under the action of sulfate and wet dry cycles Gan Lei; Wu Jian; Shen Zhenzhong; Feng Xianwei. Journal of Civil Engineering, 2021

[12] Chemo-mechanical modelling of the external sulfate attack in concrete. Nicola Cefis;Claudia Comi.Cement and Concrete Research,2017

[13] Experimental study on mechanical properties of hybrid fiber lightweight aggregate concrete Zhang Meng; Luo Wenjin. Concrete and Cement Products, 2021

[14] Accelerated sulfate attack on mortars using electrical pulse. Qian Huang;Chong Wang;Changhui Yang;Limin Zhou;Jiqiang Yin.Construction and Building Materials,2015

[15] Research on the damage model of desert sand fiber reinforced concrete under freeze-thaw cycles Zhang Guangtai; Geng Tianjiao; Lu Haibo; Wang Mingyang; Li Xuefan. Silicates

Bulletin, 2021

[16] Microstructural origins of cement paste degradation by external sulfate attack. Pan Feng;Edward J. Garboczi;Changwen Miao;Jeffrey W. Bullard.Construction and Building Materials,2015

[17] Study on the mechanical property damage of basalt fiber reinforced concrete under salt freezing action Xu Cundong; Huang Song; Li Hongfei; Li Zhen; Lian Haidong; Li Zhirui. Silicates Bulletin, 2021

[18] [12]Experiment study on the failure mechanism of dry-mix shotcrete under the combined actions of sulfate attack and drying – wetting cycles. Di-tao Niu;You-de Wang;Rui Ma;Jia-bin Wang;Shan-hua Xu.Construction and Building Materials,2015

[19] Mechanical properties and applications of basalt fiber reinforced concrete Wang Ruizhen. Residential Facilities in China, 2021

[20] Sulfate resistance of cement-reduced eco-friendly concretes. Florian Mittermayr;Moien Rezvani;Andre Baldermann;Stefan Hainer;Peter Breitenb ü cher;Joachim Juhart;Carl-Alexander Graubner;Tilo Proske.Cement and Concrete Composites,2015

[21] The damage and deterioration law of recycled concrete under the coupling effect of chloride salt freeze-thaw Jie Guoliang; Shen Xiangdong; Liu Jinyun; Zhang Bin. Silicates Bulletin, 2021

[22] A non-homogeneous model to predict the service life of concrete subjected to external sulphate attack. Chaofan Yi;;Zheng Chen;;Vivek Bindiganavile.Construction and Building Materials,2019

[23] The influence of carbon nanotube content on the mechanical properties and microstructure of concrete under the coupling effect of sulfate and freeze-thaw cycles Tang Guangsheng; Wang Feng .Hydroelectric Power Generation, 2020

[24] Study on the influence of basalt fiber length on the mechanical properties of shotcrete Wang Zhijie; Xu Cheng; Wang Jiawei; Wei Ziqi; Li Ruiyao; Xu Junxiang; Willow trees Tunnel Construction (in Chinese and English), 2020